Polymer 50 (2009) 832–844

Contents lists available at ScienceDirect

Polymer

journal homepage: www.elsevier.com/locate/polymer

Effect of comonomer type on the crystallization kinetics and crystalline structure of random isotactic propylene 1-alkene copolymers

K. Jeon [a], H. Palza [b], R. Quijada [b], R.G. Alamo [a,*]

[a] Florida Agricultural and Mechanical University and Florida State University College of Engineering, Department of Chemical and Biomedical Engineering, 2525 Pottsdamer St., Tallahassee, FL 32310-6046, United States

[b] Departamento de Ingeniería Química, Facultad de Ciencias Físicas y Matemáticas, Universidad de Chile, y Centro para la Investigación Interdisciplinaria Avanzada en Ciencia de los Materiales (CIMAT), Casilla 2777 Santiago, Chile

ARTICLE INFO

Article history:
Received 26 August 2008
Received in revised form
13 October 2008
Accepted 15 October 2008
Available online 30 October 2008

Keywords:
iPP copolymers
Crystallization kinetics
Polymorphism

ABSTRACT

Isothermal crystallization kinetics and properties related to the crystalline structure of four series of random propylene 1-alkene copolymers have been comparatively studied in this work. Comonomers studied include ethylene, 1-butene, 1-hexene and 1-octene in a concentration range up to 21 mol%. All copolymers were synthesized with the same metallocene catalyst to provide an equivalent random distribution and a similar content of stereo and regio defects within the series. This has ensured that differences in crystallization kinetics and in crystalline properties of copolymers with matched compositions reflect the affinity of the comonomer type for co-crystallization with the propene units, and the effect of content and type of co-unit in the development of the crystalline structure. In the nucleation-driven crystallization range, that is for T_cs $> T_{c\ max}$, the values of the rate follow the sequence PB > PE > PH = PO for comonomer contents <13 mol%, and PB > PE > PH > PO for >13 mol% comonomer. These trends in overall crystallization are guided by differences in undercooling due to a similar progression of the degree of participation of the comonomer in the crystalline lattice. The variation of the rates at T_cs $< T_{c\ max}$ follows the melt segmental dynamics driven by differences in T_g, especially at the highest co-unit contents, resulting in a reverse rate sequence for PHs and POs >15 mol%, i.e., PB > PE ~ PO > PH. In addition to crystallization kinetics, a comparative polymorphic analysis and unit cell expansion, crystalline morphology, and melting behavior have been instrumental in resolving the partitioning of the four types of co-units between crystalline and non-crystalline regions. 1-Butene units participate at the highest level followed by the ethylene units, as demonstrated by solid-state NMR. However, both units are defects that hinder crystallization, as given by the decreasing rates, decreased levels of crystallinity and lowered melting temperatures with increasing co-unit content. All crystalline properties of PHs and POs conform to a rejection model of the 1-octene units from the crystals in the whole compositional range, and rejection of the 1-hexene units for PH <13 mol%, a conclusion also supported by NMR. The ability of PH >13 mol% to pack comonomer-rich sequences into a stable trigonal lattice leads at T_cs $> T_{c\ max}$ to an increased number of crystallizable sequences, and to faster crystallization rates than for matched PO copolymers.

1. Introduction

Poly(propylene) and related copolymers find wide spread use in the modern day world from injection molded parts to fibers and films, with an economic impact that evolved from the 1960s to the present into the highest growth polyolefin, with a high volume production and a wide range of applications. Properties within this wide spectrum of applications are mostly tuned by the facile ability to change crystallinity via altering the chain structure of the homopolymer and/or process parameters [1,2]. An inexpensive route to alter chain microstructure is by copolymerization with relatively low contents of other 1-alkene comonomers, this lowers crystallinity and the glass transition temperature, and expands the range of applications from those requiring the stiffness and high modulus typical of the highly crystalline homopolymer to applications where elasticity and high impact are required at and below ambient temperatures. The spectrum of properties that relate to homogenous copolymers with the random distribution is primarily tuned by the content and type of comonomer, and although presently only ethylene and 1-butene comonomers are industrially used, copolymers of propylene with higher α-olefins are foreseen to be of industrial relevance and be produced in a near future due to

* Corresponding author.
E-mail address: alamo@eng.fsu.edu (R.G. Alamo).

0032-3861/$ – see front matter © 2008 Elsevier Ltd. All rights reserved.
doi:10.1016/j.polymer.2008.10.032

the versatility of property changes that a different level of co-crystallizability of the propene and the comonomer unit impart in these materials.

The above practical considerations coupled with the fact that copolymers made with single-site metallocene catalysts are now available with a uniform inter-chain comonomer composition and random intra-chain comonomer distribution have recently infused interest in understanding the crystalline properties of these types of copolymers. Major interest has been placed on understanding the effect of the comonomer as a defect on the formation of the two most common crystallographic polymorphs, the α and the γ phases, in melt-crystallized specimens [3,4]. The effect of the type of comonomer on melting, heat of fusion, and lamellar morphology in rapidly crystallized specimens of a wide compositional range has been reported recently, mainly in different publications each dedicated to a set of a fixed comonomer type [5–11]. It is important that these properties are analyzed for sets synthesized with the same catalytic system to infer the role of the type of comonomer in the crystalline properties of these copolymers. The reason is that different catalytic systems may impart a different defect microstructure and/or distribution in the copolymer chain, thus changing the crystalline properties as shown by De Rosa et al. in a recent work [8].

Notwithstanding the dedication to understand the partitioning of the comonomer units between the crystalline and non-crystalline regions and its possible impact on the α or γ crystallographic registry, none of the previous works have studied comparatively the effect of comonomer type on the isothermal crystallization kinetics of homogeneous random propylene copolymers. Given that the mechanism of crystallization of propylene random copolymers is driven by the selection of the most crystallizable sequences, differences in the rates of compositionally matched copolymers must reflect a change in comonomer partitioning. We now present this comparative study of the overall crystallization rates of sets of metallocene-made, homogeneous random copolymers with ethylene, 1-butene, 1-hexene or 1-octene comonomer units as a means to understand the role of the comonomer type in the morphogenesis of these materials, and to clarify present discrepancies in the partitioning of 1-hexene and 1-octene units. As also shown, the polymorphic structures and lamellar morphology of isothermally crystallized copolymers conform to the comonomer distribution extracted from NMR and the crystallization rates. To be used as useful materials, most of the transformation processes involving these copolymers rely on a fast crystallization from the melt state; therefore, a detailed knowledge of the crystallization kinetics sets a fundamental background for a fine tuning of the most appropriate processing properties.

2. Experimental

The iPP based copolymers studied are experimental samples free of additives, synthesized with the same bridged metallocene catalyst type in an industrial research laboratory [12,13]. Their molecular characterization is given in Table 1, and some CRYSTAF profiles are included in Supporting information. The sample designation encodes the type of comonomer and the total defect content. The type and fractional content of all the defects were obtained from solution-state ^{13}C NMR spectra. All samples are free of residual monomer as indicated by lack of the allylic methylene carbon in the spectra of PH and PO copolymers, and by lack of the vinyl group (=CH_2, 4.95–5.10 ppm and CH=, 5.8–5.9 ppm) in the proton NMR spectra. Because stereo and regio defects (of similar contents for the series studied) also affect the crystallization behavior, the analysis of experimental data throughout the text is referred to the total concentration of all types of defects, which is also listed in Table 1. The molar mass and its distribution were determined by standard gel permeation chromatography.

The original polymers were sandwiched between thin Teflon© films and compression molded in a Carver press at 180 °C to films of ~0.6 mm thick. After melting for ~5 min in the press, the films were taken at room temperature and left for 2 weeks prior to initial DSC melting. Given that the copolymers with defect contents higher than 15 mol% display rather slow crystallization kinetics at room temperature, this aging step is important to compare melting properties among the series at a stage when most of the crystalline structure has evolved. About 7 mg of these films were used for thermal analysis using a Perkin Elmer differential scanning calorimeter DSC-7 under nitrogen flow. Temperature and heat flow calibrations were carried out with indium as standard. The first heating thermogram, the cooling thermogram and the second heating thermogram were recorded at 10 °C/min. Examples are given in Figs. S2 and S3 of Supporting information.

Isothermal crystallizations were carried out either in the DSC or in controlled temperature baths. At a fixed isothermal

Table 1
Molecular characterization and glass transition temperatures (T_gs) of metallocene iPP copolymers. The comonomer type, comonomer content and content of stereo and regio defects are listed.

Sample	Comonomer type	Comonomer (mol%)	Stereo[a] (mol%)	Regio[b] (mol%)	Total defects (mol%)	$M_w \times 10^{-3}$ (g/mol)	M_w/M_n	T_g[c] (°C)
PE10.1	Ethylene	7.5	1.7	0.9	10.1	217	1.80	−15.2
PE16.9	Ethylene	14.7	1.3	0.9	16.9	196	1.92	−24.0
PE20.8	Ethylene	18.4	1.3	1.0	20.8	134	2.07	−26.1
PE22.5	Ethylene	20.8	0.8	1.0	22.5	235	2.03	−28.0
PB8.3	1-Butene	5.8	1.4	1.1	8.3	147	2.10	−8.6
PB11.5	1-Butene	9.1	1.4	1.0	11.5	189	1.98	−9.8
PB16.6	1-Butene	14.1	1.5	1.0	16.6	285	2.09	−11.0
PB21.1	1-Butene	18.8	1.3	0.9	21.1	262	2.04	−13.5
PH9.7	1-Hexene	5.4	3.1	1.1	9.7	117	2.01	−11.6
PH13.5	1-Hexene	11.0	2.0	0.5	13.5	164	2.01	−15.5
PH15.3	1-Hexene	13.2	1.8	0.3	15.3	149	1.97	−17.3
PH22.6	1-Hexene	21.0	1.4	0.2	22.6	157	2.07	−19.9
PO8.3	1-Octene	5.9	2.1	0.3	8.3	139	1.85	−12.0
PO12.8	1-Octene	10.1	2.4	0.4	12.8	113	1.85	−20.0
PO14.3	1-Octene	11.7	2.2	0.4	14.3	114	1.82	−21.4
PO17	1-Octene	13.9	2.6	0.5	17.0	133	1.92	−22.1
PO18.5	1-Octene	16.0	2.1	0.3	18.5	96	1.92	−26.8
PO20.1	1-Octene	18.0	1.7	0.4	20.1	88	1.92	−27.4

[a] Obtained as the content of mrrm pentads at 19.5 ppm.
[b] From propylene 2,1 additions of the erythro and threo types in the 34.6–34 ppm region.
[c] Glass transition temperatures measured by DSC.

temperature, the degree of transformation was followed by the change of the heat flow versus time in the DSC-7. Overall crystallization rates were obtained from the DSC exothermic peaks as the inverse of the time required for 50% of the transformation to take place (equivalent to the half time rate concept) [14]. To maximize heat transfer, the DSC was operated in conjunction with an intracooler and under dry nitrogen flow. For copolymers that developed very low degrees of crystallinity (PE22.5, PH22.6, PO17.9, PO18.5 and PO20.1), the exothermic peak could not be resolved. Here the extent of the transformation was obtained from the endotherms by measuring the enthalpy of fusion with time as described in a previous work [5]. DSC exotherms and evolution of the heat of melting with time are given in Supporting information as Fig. S4.

Ambient temperature WAXS diffractograms were taken in a slit collimated Siemens D500 diffractometer in a 2θ range of 5°–40° with filtered Cu Kα radiation as source, and operating at 30 mA and 40 kV. The isothermal crystallization of suitable samples for WAXS analysis, and collection of diffractograms at sub-ambient and above room temperature followed the same procedures described previously [5]. Peak assignments for the α and γ phases were those given by Brückner and Meille [15] and Turner-Jones et al. [16]. The fraction of the γ polymorph was calculated, after subtraction of the amorphous halo from the areas of the $(117)_\gamma$ reflection at $2\theta = 20.1°$ and the $(130)_\alpha$ reflection at $2\theta = 18.8°$, as $A_\gamma/(A_\gamma + A_\alpha)$ [5]. Extraction of peak areas from crystalline diffraction patterns and the determination of the content of γ phase using mixed Gaussian and Lorentzian peaks to fit the resulting crystalline pattern were carried out using GRAMS [17].

Solid-state ^{13}C NMR experiments were carried out on the specimens with the highest crystallinity prepared for WAXS. All spectra were obtained at ambient temperature on a Bruker DMX300 spectrometer operating at 75.5 MHz for ^{13}C and at 300.2 MHz for ^{1}H, and using a Bruker solid-state probe for 4 mm rotors under a MAS frequency of 4000 Hz. CP MAS ^{13}C NMR spectra were collected under high power decoupling using an ^{1}H nutation frequency of 83 kHz and a recycle time between acquisitions of 5 s. The contact time for cross-polarization was 1 ms. The fundamentals of the CP MAS NMR method used to isolate the spectrum of the crystalline regions have been described in previous works, and are based on the large differences in $T_{1\rho H}$ for crystalline and amorphous regions of poly (propylenes) [18,19]. A 6 ms proton spin lock was applied prior to cross-polarization in order to filter most of the protons in the amorphous regions. Consequently, the resulting spectra are strongly weighted in the crystalline component. Furthermore, a minor fraction of the unfiltered CP MAS spectrum is subtracted from the 6 ms proton spin-lock spectrum to null the remaining non-crystalline component and to obtain the crystalline spectrum. Residues in this spectrum associated with carbons pertaining to the branches give quantitative information about the degree of comonomer participation in the crystalline regions. Chemical shifts were measured with respect to tetramethylsilane at 0 ppm and using glycine's carbonyl carbon at 173 ppm as external reference.

For AFM morphology, a film (~50 μm thick) with one free surface was placed on a Linkam hot stage, heated to 180 °C for 3 min, and crystallized isothermally by rapid cooling from the melt to T_c. AFM images were recorded in an environmental JEOL 4210 scanning probe microscope using Olympus single side coated silicon cantilevers, with spring constant of ~40 N/m and a tip radius of less than 10 nm, at a resonant frequency of ~300 KHz. Topographic and phase images were simultaneously collected under ambient conditions in non-contact AC mode at a resolution of 256 × 256 pixel/line.

3. Results and discussion

3.1. Co-unit partitioning and melting behavior

The co-unit partitioning behavior between crystalline and non-crystalline regions is first analyzed by NMR for its impact in crystallization kinetics due to expected differences in $T_m°$ and the change in undercooling at which crystallization evolves. Direct characterization by solid-state NMR of the crystalline regions of PE [5,19] and PB [20] copolymers has previously indicated that both comonomers are incorporated in the crystallites as defects, with the 1-butene comonomer incorporated at higher levels than the ethylene units [20]. Similarly, the stereo mrrm and erythro 2,1 defects were also found to be partially included in the crystal regions. The degree of incorporation of the stereo defect is similar to the ethylene, while the erythro 2,1 defect presents the lowest degree of inclusion [18]. Comonomers with longer 1-alkene co-units have not yet been studied by NMR; however, WAXD of copolymers with 1-pentene (>4 mol%) and 1-hexene (>10 mol%) units also gave evidence that both units are accommodated in the crystalline regions, packing into a trigonal unit cell [10,21,22].

While there is general agreement as to the participation of the ethylene and 1-butene comonomers in the crystalline regions of iPP copolymers, the partitioning of higher α-olefins, such as the 1-hexene co-unit (in copolymer chains with ≲10 mol% 1-hexene) or the 1-octene co-unit is still controversial. Based on solution-state NMR of residues after nitric acid digestion, Hosoda et al. concluded that both co-units are incorporated in the crystal [7], while comparative analyses of thermal and morphological properties by Arnold et al. [6] and Hiltner et al. [11] concluded that these co-units are rejected. Further works by De Rosa et al. [9] on unit cell expansion and polymorphism of 1-hexene copolymers with <10 mol% comonomer were discussed as a partial inclusion of the

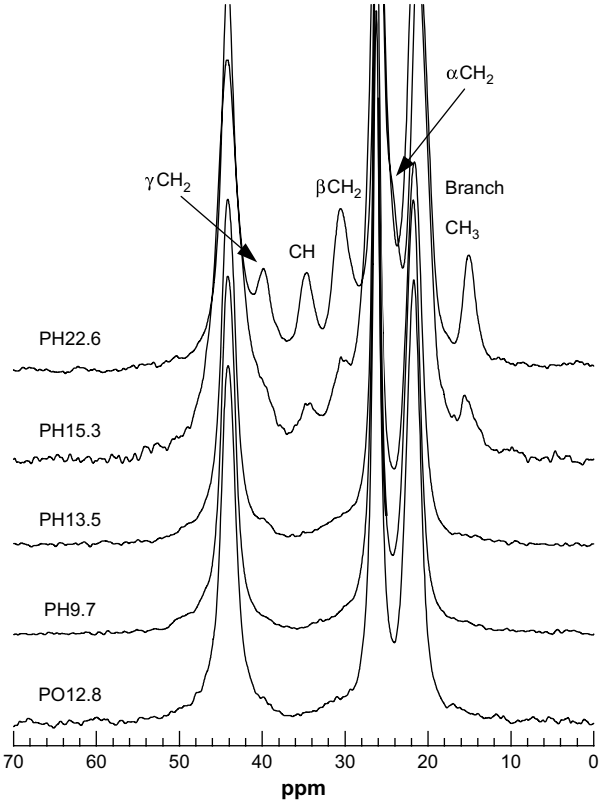

Fig. 1. Solid-state CP/MAS ^{13}C NMR spectra of the crystalline regions of PH and PO copolymers. The spectra were deduced from linear combinations of the spectra obtained with spin-lock (SL) times of 0 and 6 ms [19].

co-unit. Aiming to resolve these discrepancies, we first present a direct characterization of the crystalline regions of PH and PO copolymers by CP ^{13}C NMR.

Spectra of the crystalline regions of selected PH and PO copolymers, generated on the basis of a two-phase model following the same procedures detailed in our previous works [5,19], are shown in Fig. 1. Spectra of PO copolymers with <10 mol% 1-octene are analogous to the spectrum for PO12.8 and are not shown, while PO copolymers with >12 mol% were not analyzed due to their negligible crystallinity at room temperature. The three major resonances are associated with the isotactic propene units, methyl (~21.5 ppm), methine (~26 ppm) and methylene (~44.5 ppm), and other less intense resonances are only observed for PH copolymers with >13 mol% 1-hexene. On the basis of solution ^{13}C NMR spectra of propylene 1-hexene copolymers [23], these additional resonances are associated with carbons of the comonomer, as shown in the figure. Here the symbols α, β, and γ describe positions of CH_2 groups in side chains of 1-hexene units with respect to their CH groups (also shown). These NMR spectra corroborate the inclusion of the 1-hexene units in the crystals of PH copolymers with 1-hexene content greater than 13 mol%. This is the 1-hexene content above which a change in crystallographic unit cell from the α phase to a trigonal packing occurs due to the incorporation of the comonomer [11,21,22]. Lack of these resonances in the spectra of PH copolymers with 11 mol% (PH13.5) or 5.4 mol% 1-hexene (PH9.7) is indicative of a negligible incorporation of 1-hexene in the crystals of PH copolymers with less than 13 mol% 1-hexene. Resonances associated with the hexyl branch are not found in any of the PO crystal spectra studied here, thus suggesting exclusion of the 1-octene co-unit from the crystals of PO copolymers.

The concentration of 1-hexene within the crystalline regions was calculated from the areas of the best resolved b-CH_3 and b-CH peaks in reference to the total methyl and methine crystalline areas. The average values obtained are 5.8 and 16.1 mol% for PH15.3 and PH22.6 respectively. From these data, the partitioning coefficient P_{CR} defined as the ratio between the concentration of defects in the crystal with respect to the concentration of defects in the chain is compared in Table 2 for the most common iPP defects and α-olefin comonomers. For a relatively low defect concentration, $\lesssim$3 mol%, these data indicate that the 1-butene co-unit has the highest co-crystallizability with the propene unit, followed by the ethylene and stereo mrrm defect with a similar effect, and by the 2,1 erythro defect. The 1-pentene and 1-hexene co-units are special cases of incorporation of comonomer-rich segments into a trigonal iPP crystal structure when the concentration of the comonomer is >4 mol% or >10 mol% respectively [10,21]. Since resonances associated with the butyl branch are only found in the crystalline spectra of PH copolymers that crystallize partially or totally in the trigonal form, the initial conclusion is made that 1-hexene units are only accommodated in trigonal crystals and are excluded from the α or γ phases. This explains the relatively sharp comonomer transition for the formation of trigonal phase in PH copolymers, suggesting a threshold in the sequence length distribution of the random copolymer to enable crystallization of sufficient comonomer-rich segments, with butyl branches spaced by only few propene units, to allow crystal growth with the suggested trigonal structure [10].

Table 2
Partitioning coefficient, P_{CR}, of defects found in iPP and propylene copolymers. P_{CR} is defined as the ratio between the concentration of the defect in the crystal over the concentration of defect in the chain.

Defect type and content	P_{CR}[b]
1,3 (2.4 mol%)	0.0 [18]
2,1 erythro (≤1.0 mol%)	0.27 ± 0.03 [18]
mrrm stereo (≤2.0 mol%)	0.48 ± 0.03 [5,18]
Comonomer: ethylene (1–21 mol%)	0.45 ± 0.03 [5,19]
1-Butene (<3 mol%)[a]	0.55 ± 0.04 [20]
1-Hexene (≤11 mol%)	0.0
1-Hexene (13.2 mol%)	0.44 ± 0.02 [this work]
1-Hexene (21 mol%)	0.77 ± 0.03 [this work]
1-Octene	0.0 [this work]

[a] P_{CR} is expected to increase for 1-butene contents >3 mol%.
[b] Values in brackets are citations.

Differences in comonomer partitioning, given by the data of Table 2, are reflected in the comparative melting (T_{mf}) and heat of fusion (ΔH) behaviors in Fig. 2 where data for copolymers with total defects <8 mol% studied in a previous work [3] are also included. The decrease of T_m and ΔH with increasing comonomer content has been well documented so that this matter is not of current concern. The interest is the effect on melting of the type of unit for random samples made with a single-site metallocene catalyst. For this purpose, we plot the final melting temperature of the endotherm (T_{mf}), instead of the melting peak because it is at the T_{mf} value when the composition of the melt most closely resembles the defect chain composition for any copolymer. Due to the coexistence of the alpha and gamma structures in most iPP copolymers, and the higher melting of the alpha phase [3,24], plotting T_{mf} for copolymers with <15 mol% defects also ensures that the melting behavior of the same alpha structure is comparatively analyzed for these copolymers. At a fixed comonomer composition, copolymers with the most co-crystallizable co-unit (PB) melt at the highest temperatures, followed by PE, and further by PH and PO. Up to a defect content of 15 mol%, the melting behavior of PH and PO copolymers is equivalent, indicating that both co-units must behave in a very similar way with respect to the incorporation into the crystal lattice. Hence, this melting data support the NMR results indicating that in this compositional range the 1-hexene and 1-octene co-units cannot enter the iPP lattice to any meaningful extent in melt-crystallized systems. Compared to PH and PO copolymers, PBs and PEs of a matched composition have longer and a higher fraction of crystallizable sequences that may lead to thicker crystallites. Consequently, the melting temperatures and heat of fusions are higher, as experimentally observed in Fig. 2a and b. The melting variation of these copolymers is also explained on the basis of phase equilibrium between crystallites of the same α nature and a composition dependent melt. The comonomer composition of the melt coexisting with PH and PO crystals is richer than the corresponding PE or PB crystallites formed from copolymer chains with matched compositions. Therefore, on equilibrium basis, and in reference to the homopolymer, the melting of PO and PH crystallites is more depressed than the PE or PB melting. The apparent invariance of the melting temperatures of PH and PO copolymers in the 17–23 mol% range is due to the slow crystallization kinetics at room temperature, such that the values reflect melting of isothermally formed and aged crystallites at 23 °C.

While the heat of fusion of PO copolymers decreases linearly from 85 to 5 J/g with comonomer up to about 20 mol%, PH copolymers follow the same linear behavior only up to ~13 mol% comonomer. For higher 1-hexene contents the heat of fusion of PH is higher, even greater than the value of matched PEs. This behavior was first described by Poon et al. [11] and is attributed to the participation of 1-hexene and propene units in crystallites with a different, denser structure, a trigonal phase [21,22]. Since the heat of fusion of the pure trigonal structure is unknown, one cannot conclude from these data that the degree of crystallinity of PH22.6 is higher than the value for PE or PO with a matched comonomer content, this issue is better resolved by WAXS analyses, as shown later.

The variation of the glass transition temperature for the same copolymers, measured by DSC, is given in Fig. 2c. As these data relate to segmental mobility, the differences observed between the

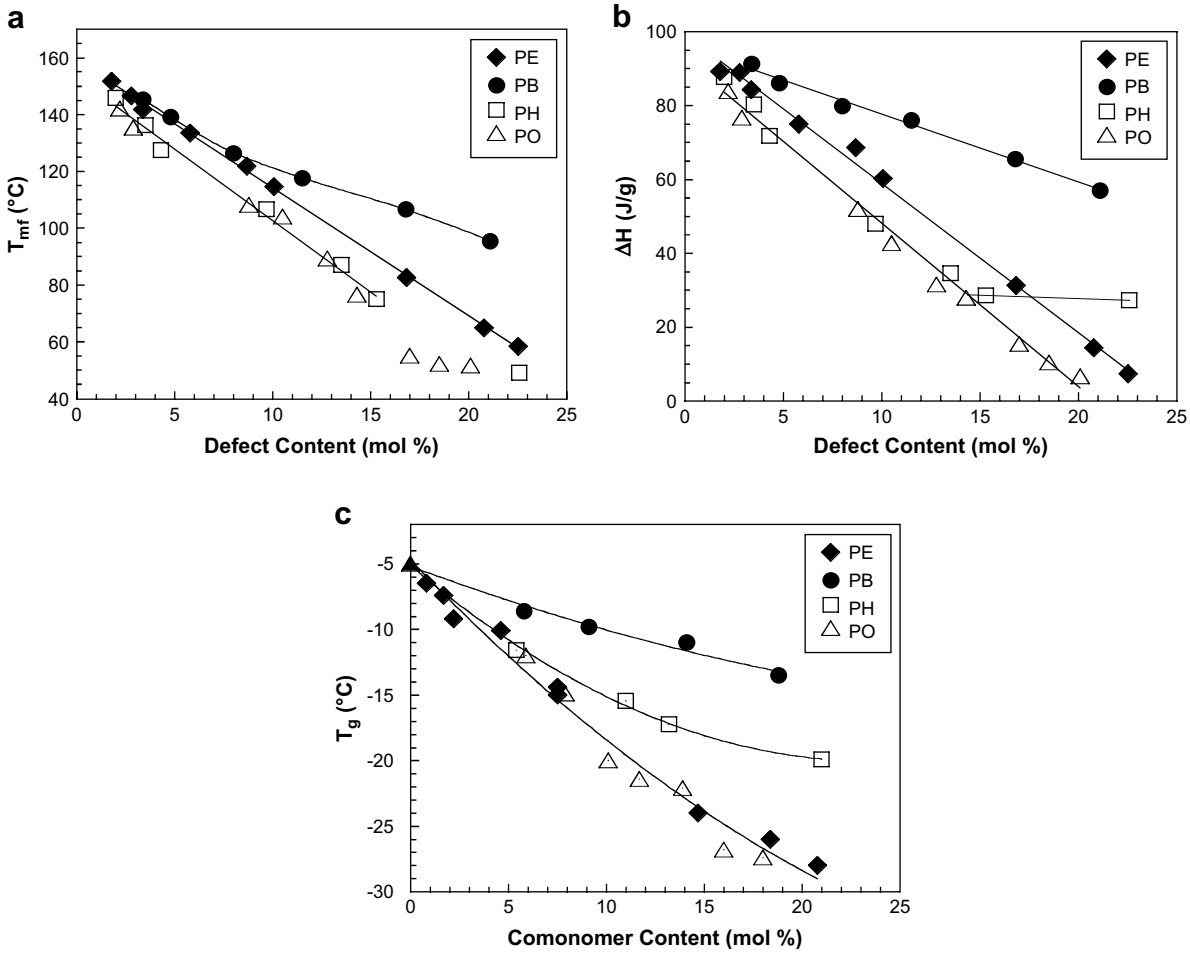

Fig. 2. Thermal properties as determined by differential scanning calorimetry for copolymers melt crystallized at 23 °C, and kept at RT for 2 weeks. (a) Final melting temperature (T_{mf}), and (b) heat of fusion (ΔH) versus total defect content. (c) Glass transition temperature as a function of comonomer content. Lines are drawn to guide interpretation of the experimental data.

four copolymer types are important to describe their crystallization kinetics, especially for data obtained in a temperature range where the kinetics are driven by segmental transport. T_g decreases with increasing co-unit content as a consequence of the plastification effect conferred by the comonomer and the increased free volume. The trend with increasing branch length from PB to PO is the same as observed by Arnold et al. [6], and Dlubek et al. [25] in similarly constituted copolymers. Of interest in the data of Fig. 2c is the variation of T_g for PEs, not studied in the works of Arnold and Dlubek et al., that shows similar values to those of PO copolymers. When comparing T_g values of PEs (from −12 to −27 °C) and PBs (from −8 to −13 °C), higher values in the PB series reflect the steric hindrance caused by branching to segmental motion, and when comparing the PB–PH–PO series at a fixed co-unit content, the decrease of T_g is associated with the increased flexibility of the linear side chain as branch length increases from two to six carbons.

3.2. Overall crystallization kinetics

The isothermal crystallization rates are next analyzed in reference to their sensitivity to changes in content and length of crystallizable sequences in random copolymers as the co-unit is totally or partially discriminated from the crystalline regions. The rates associated with the inverse of the time required to acquire half of the transformation are given in Fig. 3. For clarity of presentation, rate data are comparatively shown for PE and PB copolymers in Fig. 3a, while data for PH and for PO are given in Fig. 3b. The rates of PEs are taken from a previous work [5].

In the compositional range studied, up to ∼20 mol%, PEs, PHs and POs with comonomer contents >15 mol% (PE) and >10 mol% (PH and PO) respectively, show a maximum of the crystallization rate with increasing T_c. This is due to the shift to lower values of the accessible T_c interval to observe crystallization kinetics with increasing comonomer content, as detailed in our previous work [5]. Given that in these copolymers the co-unit is partially or totally rejected from the crystalline regions, T_m° is predicted to decrease with increasing comonomer, sufficient sequences of the required length for crystallization are only found at undercoolings corresponding to much lower T_cs, those approaching T_g for these copolymers. Since the available number of sequences for crystallization is increasingly restricted with increasing comonomer content, the result is slow kinetics and a reduced level of crystallinity due to the limited number of crystallizable sequences and transport limitations that reduce further the availability to propagate crystal growth.

A quantitative assessment of differences in the crystallization rates within the series, and for increasing comonomer content would require an independent kinetic analysis of the two different crystallographic phases that develop simultaneously for many of these copolymers [3,5,26,27]. On this subject, we found out from previous work [3] that α and γ have the same initial crystallization rates. Therefore, the possible contribution of differences in kinetics is minimized at the early stages of the transformation. However, the

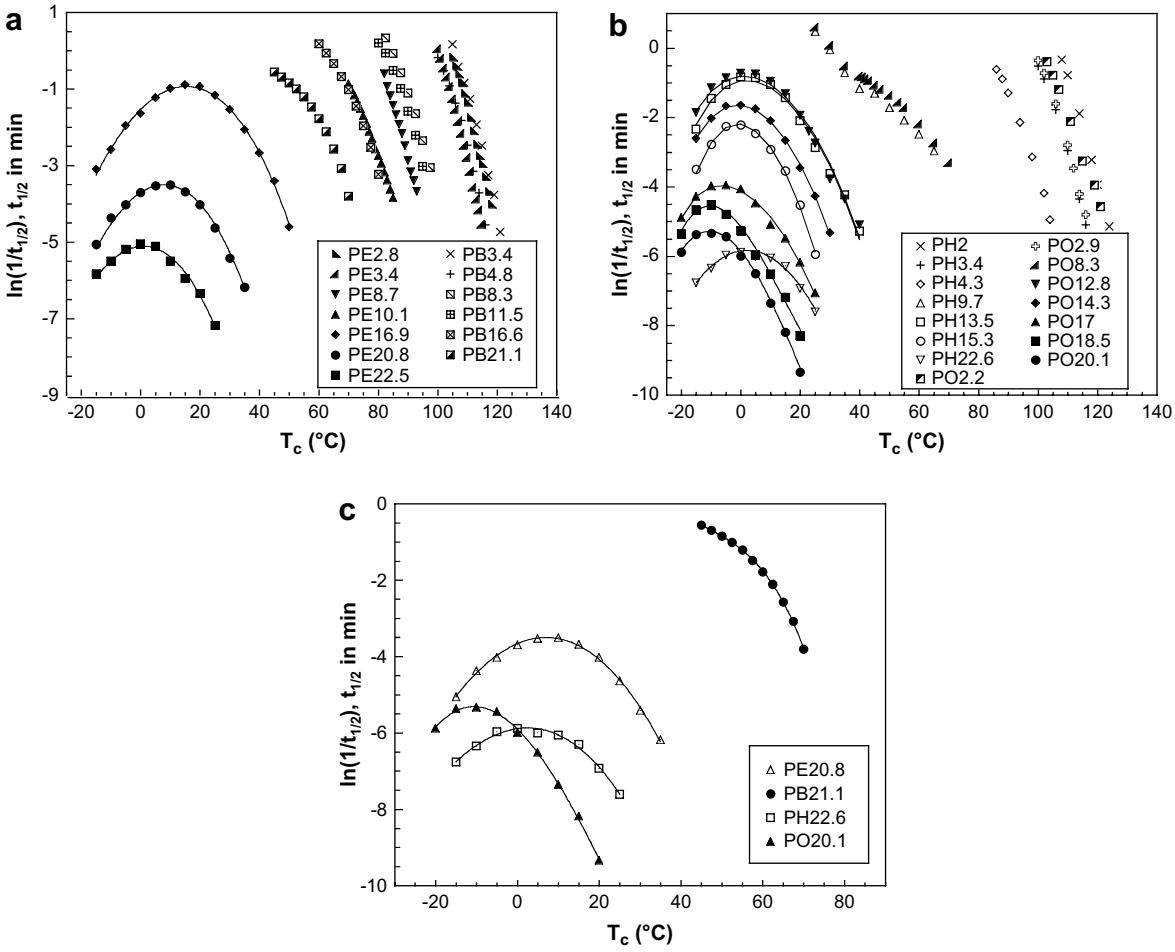

Fig. 3. Overall crystallization rate expressed as $\ln(1/t_{1/2})$ as a function of crystallization temperature (T_c) for (a) PE and PB copolymers, (b) PH and PO copolymers, and (c) PE, PB, PH and PO copolymers with ~20 mol% comonomer. Solid lines are drawn over experimental points for visual aid.

rate data on the basis of a small transformation, for example the time to reach 10% of the transformation, lead to identical trends to those of Fig. 3. Furthermore, in the nucleation controlled T_c range, the analysis should be carried out at the same undercooling rather than for the same T_c, as shown in Fig. 3. Comparing the rates of compositionally matched copolymers at the same undercooling ($T_m^\circ - T_c$) will account for differences in T_m° due to the diverse partitioning behavior of the co-unit. However, this comparison is difficult in these complex series because values of T_m° for many of the copolymers are unknown. Even an estimation of T_m° using equilibrium-based formalisms for random copolymers with co-units excluded [28] or included [29] in the crystal requires parameters such as the heat of fusion, ΔHu, which is likely to change from the value of the homopolymer as the comonomer increases, especially when the comonomer participates in the crystal. A possible change of Δ*H*u is also unknown. Due to these limitations, the overall rates will be first discussed for matched T_cs, with inference to a change in undercooling as the major parameter leading to differences in rates obtained at high T_cs. At T_cs approaching T_g growth is dominated by segmental transport, and hence by melt viscosity instead of undercooling.

At any fixed T_c, the crystallizations of PBs are faster than for matched PEs (Fig. 3a). This is the expectation from the relatively high co-crystallizability between the propene and 1-butene units, as shown by NMR and melting data. PBs have longer and a greater number of crystallizable sequences than analogous PEs because more of the 1-butene co-units can participate in the crystalline lattice. It is thus expected that, for crystallizations at the same T_c, PB copolymers crystallize at much higher undercoolings than matched PEs. Due to fast kinetics, the maximum of crystallization rate is not observed for PB copolymers even at 1-butene contents of ~20 mol%. The differences in crystallization rates between PEs and PBs greatly accentuate with increasing comonomer, and while below 5 mol% defects PBs crystallize at double the rate of PEs, the rates of PB16.6 are over 1000 times faster than the analogous PE16.9, and match those of PE10.1, a propylene ethylene with much lower comonomer content.

The crystallization rate behavior of PHs and POs, shown in Fig. 3b, is also explained in reference to the partitioning of both units and the values of T_g for these copolymers. At a fixed T_c the rate of compositionally matched PH or PO copolymers is lower than the data for PB or PE copolymers as expected, due to differences in co-unit partitioning, as shown in Table 2, and the expected depletion in number of crystallizable sequences with the required length in PHs and POs. Up to a defect of 15 mol%, PH and PO copolymers display very similar overall crystallization. For example, the rate of PH3.4/PO2.9, PH9.7/PO8.3 and PH13.5/PO12.8 practically overlaps between the pairs. The difference in overall rate between PH15.3 and PO14.3 is attributed to a larger mismatch in comonomer content. As listed in Table 1, PH15.3 has 1.5 mol% higher comonomer than PO14.3, and hence, lower crystallization rates. We then conclude that up to 15 mol% the crystallization rates of PH and PO conform to the NMR and melting results that indicated that both co-units are rejected from the lattice in this compositional range.

Significant differences in kinetics between PH and POs are only found for >15 mol% defects (≳13 mol% comonomer) as shown in

Fig. 3c where the isothermal crystallization rates are compared for the four types studied at the same ~20 mol% comonomer and for similar molecular weights. Matching molecular weights of PE, PH and PO, in addition to co-unit, is important at this level of defects, because, as discussed in an earlier work, crystallization is only observed at T_cs close to T_g where viscosity plays a dominant role in the rate. With respect to PB, the crystallization rates decrease quite abruptly for PE, PH and PO, indicating the reduced availability of segmental sequences that can participate in the nucleation and growth processes of these three copolymers. Of interest is the unique comparative rate behavior on both sides of the maximum. At $T_c > 5$ °C above the $T_{c\ max}$, PE crystallizes faster, followed by PH and by much lower rates of PO, while at $T_c < -5$ °C, below $T_{c\ max}$, the rates of PE and PO are similar while the rate of PH is significantly lower. The temperature dependence of the rates is readily explained considering how the type of comonomer affects the change in free energy for nucleation (ΔF^*) and segmental transport (ΔE_D) which are the major drives for crystallization above and below $T_{c\ max}$, as given by the Turnbull–Fischer equation for the nucleation rate [30]:

$$N = N_0 \exp\left[-\frac{\Delta E_D}{RT} - \frac{\Delta F^*}{RT}\right]$$

In the high T_c range, the rate data for PH22.6 are higher than for PO20.1 following the increased number of crystallizable sequences of PH at this compositional level due to the participation of the 1-hexene units in the crystal. In reference to the data for PO20.1, the kinetic data of PH22.6 point to a higher T_m°, as expected for the trigonal unit cell that accommodates the 1-hexene units in a structure with higher packing density, as compared with the monoclinic (α phase) of PO20.1 free of co-units. Clearly in the high T_c range, the rates follow the degree to which the co-unit participates in the crystallites. We do not find any PO with faster kinetics than PH in this temperature range, as stated in the work of Poon et al. [11] (see Fig. 9 of this work), nor this is expected since NMR and other PO properties suggest that the 1-octene unit is always excluded from the crystal, while the 1-hexene unit may not be. It is possible that the PH and PO copolymers compared by Poon et al. were made with different catalysts, and had different contents of stereo and regio irregularities. This could impact the rates to a larger extent than the difference due to the co-unit. This feature reveals again the importance that properties are compared for copolymers synthesized with the same metallocene catalyst under the same conditions in order to draw sound conclusions on the effect of comonomer type on crystallization.

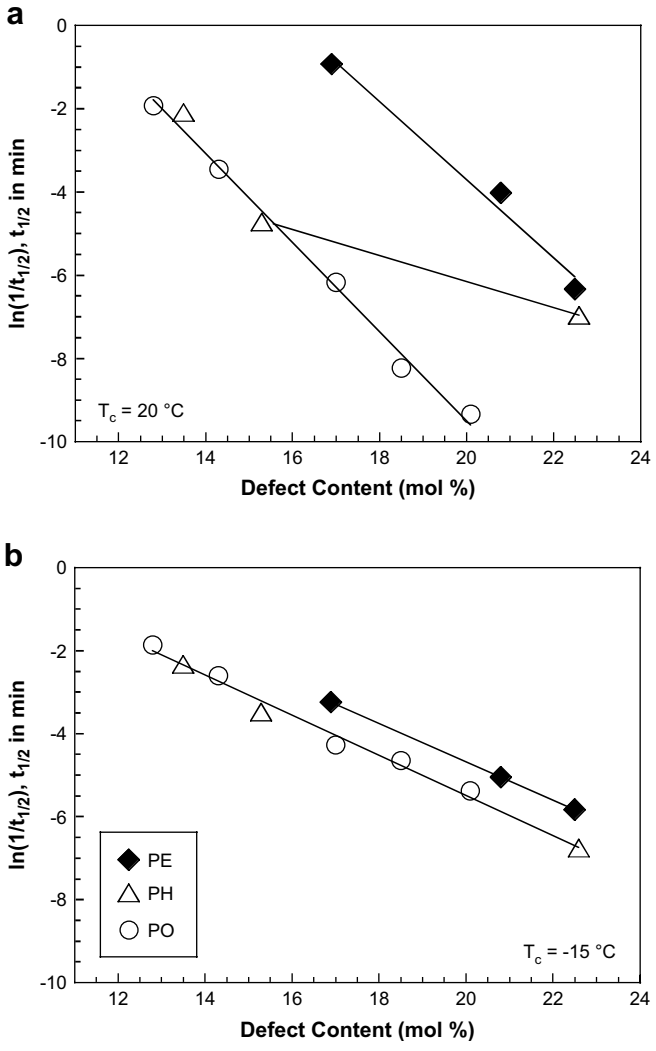

Fig. 4. Overall crystallization rate as a function of defect content for PE, PH and PO copolymers isothermally crystallized at (a) 20 and (b) −15 °C.

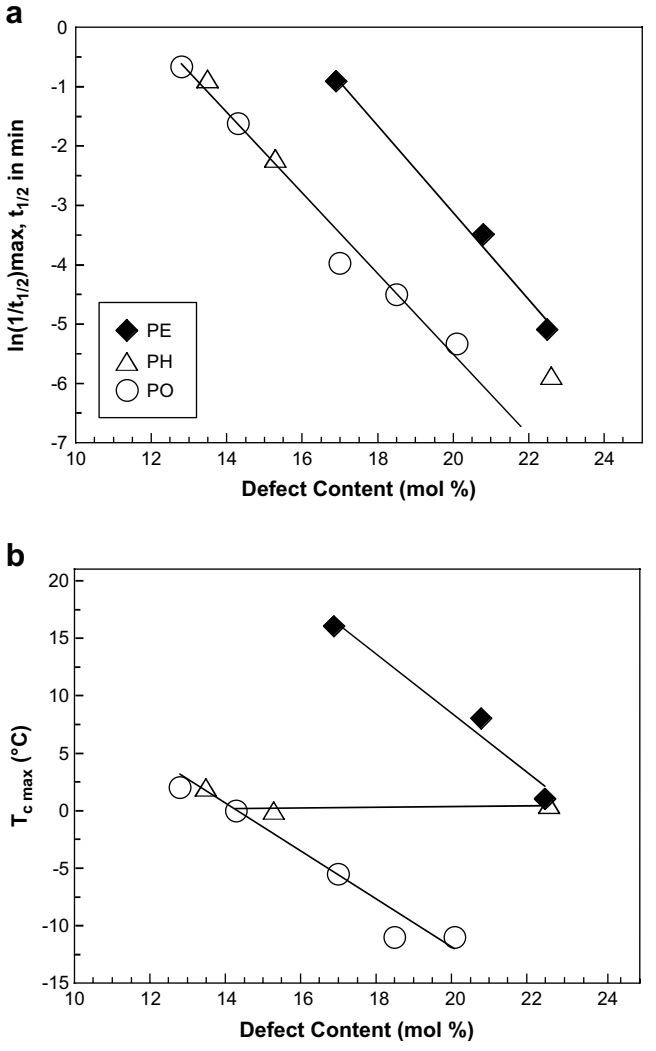

Fig. 5. (a) Maximum value of the rate and (b) temperature ($T_{c\ max}$) at rate maximum as a function of defect content for PE, PH and PO copolymers.

The values of the rates of PH and PO to the left of $T_{c\,max}$ follow an opposite trend. Here the rates of PO are higher than those of PH, and the rates of PO and PE overlap at the lowest T_c studied. This trend with decreasing T_c parallels the variation of T_g in these copolymers, a parameter that impacts the free energy change for segmental transport (ΔE_D), and crystallization kinetics, at temperatures so close to T_g. As seen in Fig. 2, PO and PE have very similar T_g values, hence, the crystallization rates at $T_c < -10\,^{\circ}C$ are also very similar. Conversely, the T_g of PH22.6 is $\sim 10\,^{\circ}C$ higher, making ΔE_D at low T_cs also higher, and leading to lower rates than for matched

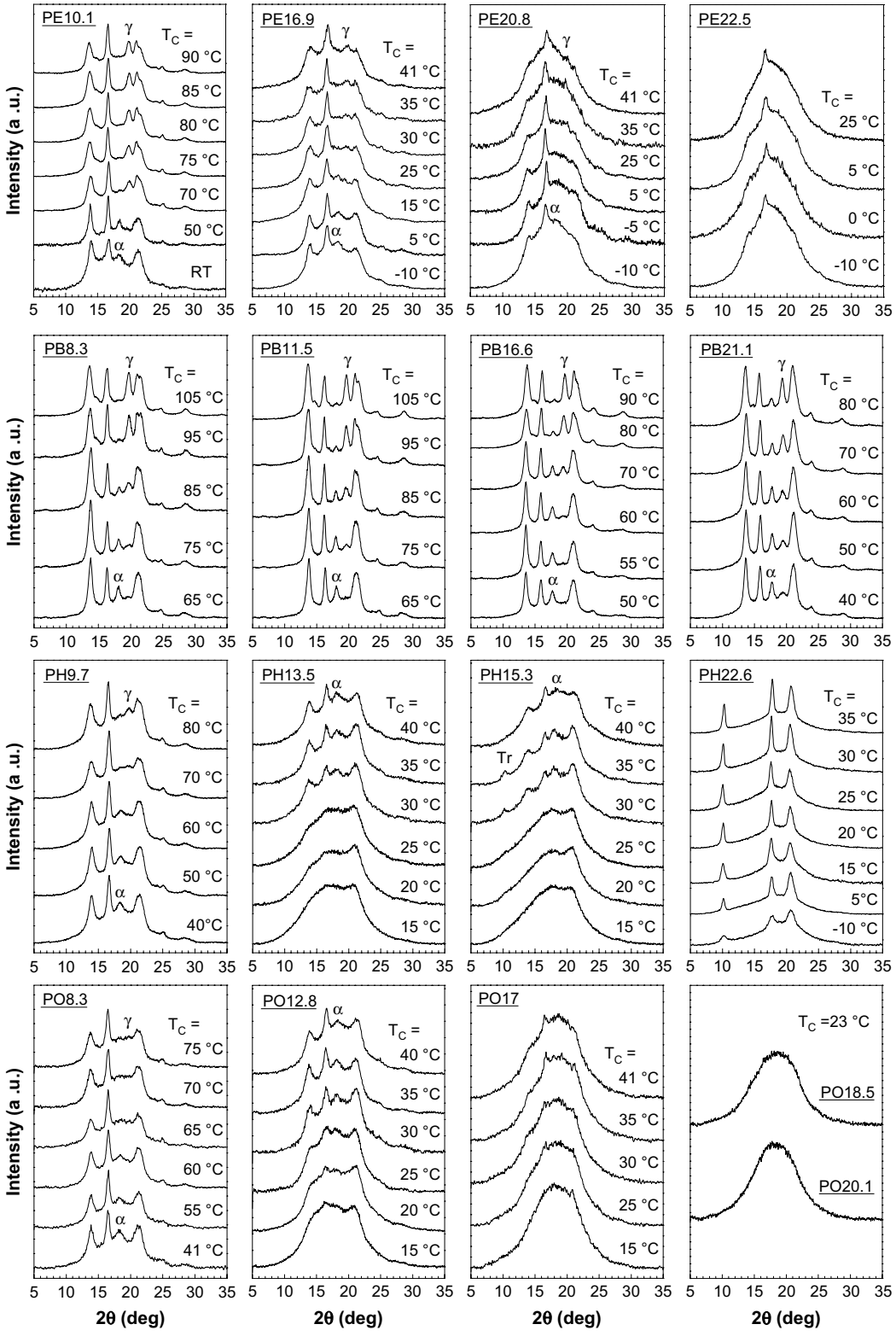

Fig. 6. Powder WAXS diffractograms of the four copolymer series isothermally crystallized at the indicated temperatures. Reflections corresponding to the α (2θ ~ 18.6°) and γ (2θ ~ 20.0°) polymorphs are indicated. The reflection marked as "Tr" in the profile of PH15.3 indicates a trigonal crystal structure. Diffractograms of copolymers crystallized at T_cs below 15 °C were obtained at the crystallization temperatures using a Peltier cell.

PEs or POs. At T_cs near T_g the increased number of crystallizable sequences from the inclusion of l-hexene in the crystal lattice of PH22.6 is not the limiting parameter for nucleation and growth. At these T_cs the barrier for nucleation is low, but transport restricts crystallization. Here, a higher ΔE_D value for PH22.6 limits segmental transport compared to the melt dynamics of matched PE and PO.

The different behavior of crystallization rates in the nucleation controlled T_c range as compared to those obtained in the segmental transport driven range is summarized in Fig. 4. Here the isothermal rates obtained at extremes T_cs of the bell-shape, i.e., 20 °C and −15 °C, are plotted as a function of defect content for PE, PH and PO copolymers (notice that the fast kinetics of PB can not be compared at these T_cs). At 20 °C, in the nucleation controlled T_c range, and for <15 mol%, the rates of PEs are ~150 times faster than for PO or PH copolymers, in accordance with the inclusion of ethylene and exclusion of 1-hexene and 1-octene from the crystallites. When the 1-hexene unit is included, such as for PH >15 mol%, the crystallization is faster and at ~20 mol% approaches the value of a PE with double molar mass due to the large incorporation of l-hexene units in this compositional range. In contrast, when crystallization is carried out at −15 °C the difference in kinetics between PE and PH and PO is minimized as seen in Fig. 4b. At $T_c = -15$ °C, the influence of co-unit content on decreasing the crystallization rate follows a linear behavior of about half the slope of the PE and PO data at 20 °C. As mentioned earlier, at this T_c the rate of PH22.6 does not deviate upward from linearity due to the relatively high T_g.

The temperature at which the rate is a maximum and the maximum value of the rate also follow a linear decrease with increasing comonomer content, except for PH22.6, as illustrated in Fig. 5(a) and (b). These data also demonstrate quite clearly that up to ~15 mol% comonomer PH and PO follow the same crystallization behavior, while the maximum rate values for PEs of matched compositions are significantly higher, reflecting a crystallization at higher undercoolings from the partial accommodation in the crystal of the ethylene units. In comparison, a high T_g and a possible high T_m° for the more dense trigonal structure are the major factors for the drastic increase in $T_{c\,max}$ of PH22.6 (>15 °C) compared to the PO values. Conversely, POs, PEs and low co-unit content PHs have similar T_gs, but the $T_{c\,max}$ of PEs are ~20 °C higher, suggesting higher T_m° values for PEs, as discussed earlier. Therefore, the general conclusions made from NMR and from the analysis of the crystallization rates are also in line with the observed variation of $T_{c\,max}$. PH and PO copolymers up to ~15 mol% have an equivalent behavior, and hence both co-units must have the same behavior with respect to incorporation into the crystal lattice. The results from NMR and lack of discontinuity in kinetics of the PO series with increasing comonomer content indicate that 1-octene units do not enter the lattice; accordingly, the l-hexene units at <15 mol% must be also rejected.

3.3. Polymorphism

In an earlier study that analyzed the polymorphic behavior of metallocene iPP copolymers in a relatively low range of comonomer content (<8 mol%), we concluded that the development of the γ polymorph is a good indicator of differences in the partitioning of the comonomer units [3]. The conclusion was based on experimental data indicating that short crystallizable sequences favor the formation of the γ polymorph, and holds when the copolymers are synthesized with the same catalyst and have the same random comonomer distribution [3]. The participation of a co-unit in the crystal extends naturally the length of crystallizable sequences in PB and PE copolymers, which were found to develop less of the γ phase than PHs and POs at comparable comonomer levels. However, the initial expectations with respect to the chain microstructures needed for crystal development in pure γ phase are not fulfilled when the crystal structure is analyzed in an extended compositional range, as shown in recent works by De Rosa et al. [8,9]. For example, these authors nicely demonstrated that the inclusion of large contents of 1-butene units in the crystal expands the α lattice to levels such that the γ phase can no longer be formed. This occurs because in iPP crystals formed with high 1-butene levels the a and c axial lengths lose their equivalence, a requirement for homo-epitaxy and for the development of the γ phase. They also found that the γ phase does not form in PH copolymers with 10–15 mol% 1-hexene. This unexpected feature was attributed to a small expansion of the α lattice of PH crystals formed in this compositional range. By analogy to the behavior of PB copolymers and the unmistakable participation of the 1-hexene units at levels >15 mol%, the expansion was identified with the participation of the 1-hexene units in the a crystals [9]. The conclusions by De Rosa et al. of 1-hexene inclusion in PH copolymers (<15 mol%) clearly diverge from the NMR, melting and crystallization kinetics of the series studied here. If indeed the 1-hexene units are included in the crystals and the 1-octene are not, then PH and PO copolymers with <15 mol% co-unit should show different

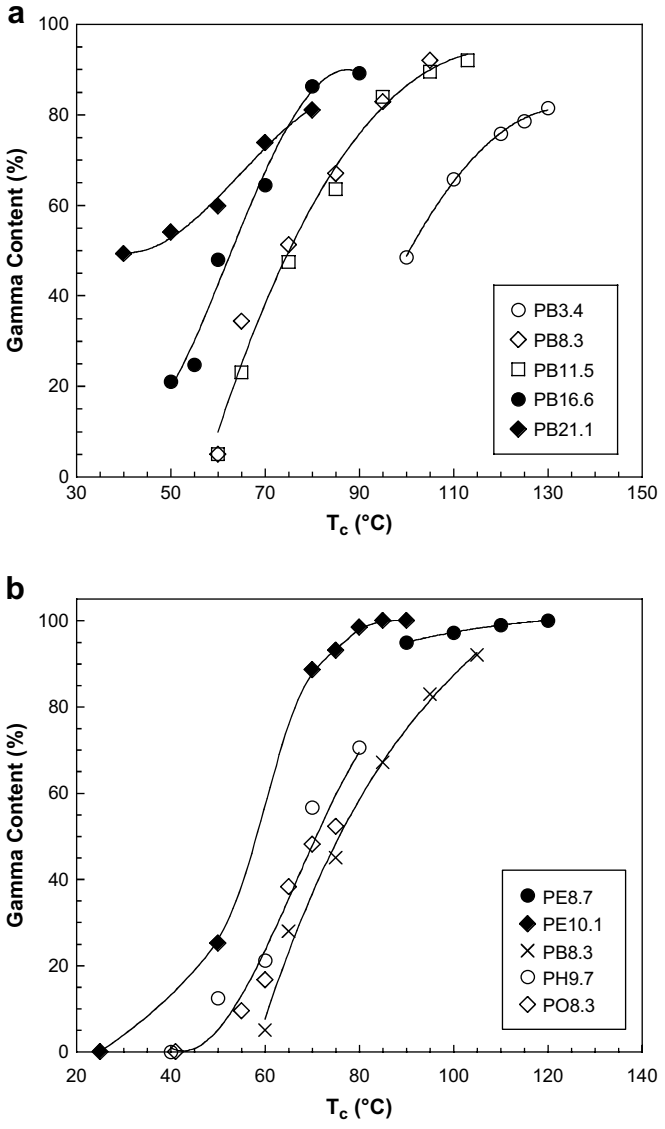

Fig. 7. Percentage of γ polymorph as a function of crystallization temperature (T_c) for (a) PB copolymers and (b) comparison between PE, PB, PH and PO copolymers with 9 ± 1 mol% defects.

polymorphism and a different level of unit cell expansion. To analyze possible differences in polymorphic behavior and lattice expansion between PH and POs, WAXD diffractograms of isothermally crystallized specimens were collected for the same copolymer series studied here. The diffractograms are shown in Fig. 6 for an extended range of T_cs, including patterns obtained at temperatures close to T_g, not studied in previous works [8,9,11].

Diffractograms for PEs and PBs with increasing T_c and increasing comonomer content are given in the two first rows of Fig. 6. The structural information obtained from these diffractograms is the same or very similar to other works [8]. However, they are included to present a complete set of structural information as the length of the 1-alkene co-unit increases. Polymorphic differences between these copolymers are, thus, more directly observed. In the co-unit range studied here, at a fixed T_c, the development of the γ phase is enhanced in both PE and PB copolymers with increasing comonomer content, following the general concept that the increase in short crystallizable sequences favors the formation of the γ phase. Only PB21.1 develops less than expected γ content at T_cs >60 °C (Fig. 7a), in agreement with the impact of a higher fraction of 1-butene incorporated in the α crystals, shown by De Rosa et al. [9].

Crystallization temperature dependent diffractograms of PHs and POs are presented in a range of ~8 to ~23 mol% defects in the third and last rows of Fig. 6. In agreement with the melting and crystallization rates, the polymorphic behavior of PH and PO up to ~15 mol% is basically identical. PH9.7 and PO8.3 crystallize in a pure α phase at the lowest T_cs and progressively develop crystals in the gamma phase with increasing T_c. This behavior was observed for lower comonomer contents in all types of iPP copolymers and has been explained as the interplay between the formation of a phase that is kinetically favorable (α phase formed at high undercoolings) and the thermodynamically more stable γ phase, thus activated at higher T_cs [3]. Given that γ does not develop at T_cs $< T_{max}$ in any of the systems studied, the additional conclusion that segmental mobility is required in addition to short crystallizable sequences to develop the γ phase [5] appears general for all iPPs and their copolymers.

The fractional content of γ phase developed by PH and PO with ~9 mol% defects is, however, lower than expected as found comparatively with respect to the content of γ phase developed by matched PEs and PBs (see Fig. 7b). While at a fixed T_c the γ content of PB8.3 is lower than for matched PEs, as expected, the content of γ found for PH9.7 and PO8.3 is basically the same value for these two copolymers but lower than for matched PEs notwithstanding the increased number of short crystallizable sequences in PH and PO copolymers. Since all properties point towards the exclusion of both higher α-olefins from the lattice at this comonomer level, the reason cannot be associated to the comonomer inclusion, as given in the earlier work [9]. The crystallographic behavior of PH13.5 and PO12.8 is also atypical because they do not develop the gamma

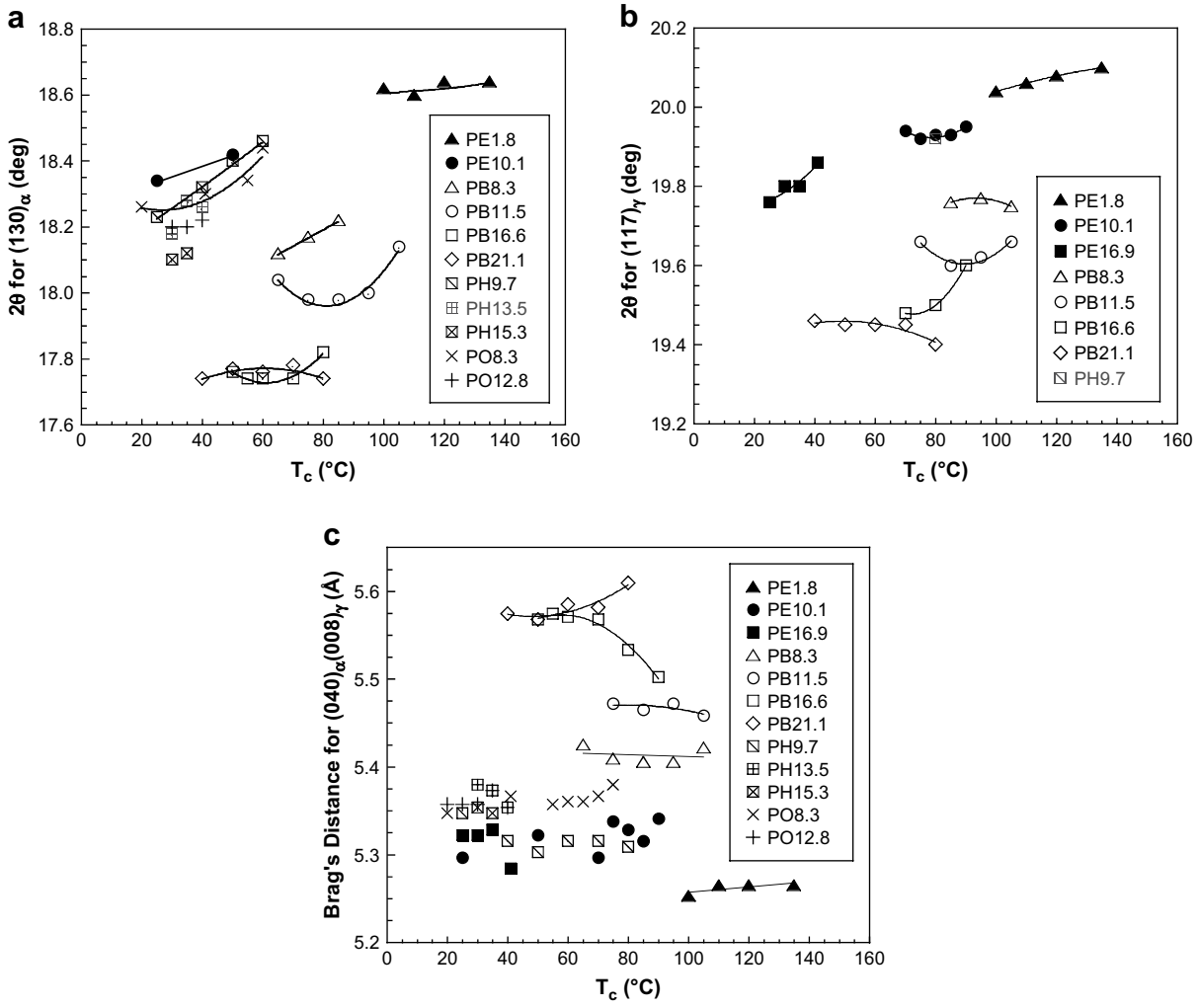

Fig. 8. Variation of 2θ peak position as a function of crystallization temperature (T_c) taken from diffractograms of Fig. 7 for (a) pure alpha reflection, $(130)_\alpha$, and (b) pure gamma reflection, $(117)_\gamma$. (c) Values of Bragg distances at $2\theta \sim 16.5^\circ$ corresponding to periodicities between $(040)_\alpha$ and $(008)_\gamma$ planes.

phase at all as seen in Fig. 6. It is quite clear that the l-octene comonomer is too large to be accommodated in a trigonal structure similar to that formed by PH22.6, and only develops small and defected crystallites at >18 mol% as reflected by the lack of crystallographic reflections at this comonomer level. Therefore, if the l-octene defect is too large to participate in a crystal lattice, then the l-hexene unit must also be excluded in the crystals of PH copolymers with ≲13 mol% comonomer (<15 mol% total defects in the series studied here), because in this co-unit range both copolymer types display the same crystallization and melting behaviors.

We have analyzed the expansion of the unit cell comparatively for the four sets of copolymers for consistency between PHs and POs in the co-unit range where both types present an equivalent crystallization behavior. The results for isothermally crystallized samples are shown in Fig. 8(a)–(c). The 2θ values characteristic of the (130) plane for the α reflection at ~18° and of the (117) plane for the γ reflection at ~19.8° are given in Fig. 8a and b. We find that only PB copolymers show at any T_c a significant decrease in 2θ (equivalent to lattice expansion) with increasing l-butene content, in consonance with inclusion of the 1-butene comonomer in both α and γ polymorphs, and in agreement with De Rosa et al.'s results [8]. The homopolymer and PE1.8 have the highest 2θ values, and the $(130)_\alpha$ and $(117)_\gamma$ reflections of PH and PO copolymers are above any PB data. There is a very small variation of 2θ (18.3 + 0.1 for the α phase) among the PH and PO data, with the exception of PH15.3 which was found to develop some trigonal phase that, as is known, includes the comonomer. The 2θ reflections of PO8.3, PH9.7, PO12.8 and PH13.5 are basically the same indicating, in parallel with previous analyses, that both co-units are rejected from the crystallites. Data for the Bragg distance of planes $(040)_\alpha$ and $(008)_\gamma$ at $2\theta \sim 16.5°$, given in Fig. 8c, lead to the same conclusion. This distance reflects direct changes in the dimension of the *b* and *c* axes of the α and γ crystals respectively. As shown, there is a negligible lattice expansion with T_c for most copolymers, while clear differences are observed in the lattice dimensions of the PB series compared to all other copolymers. The axial distance increases from 5.40 to 5.60 Å in the range of l-butene from ~5 to ~20 mol% respectively, due to the increased participation of the 1-butene units in the crystal [8]. The variation of this distance for PE, PO and PH is narrower, from 5.30 to 5.38 Å. Moreover, compared to the homopolymer and with PE data, PO and PH show the same negligible b_α and c_γ axial expansion, again indicating that the volume of the butyl and hexyl branches is too large to be tolerated in the α or in the γ crystal lattices.

Since the unit cell dimensions do not support co-unit inclusion, the lower than expected contents of γ in PH and POs at ~8 mol% co-unit or lack of formation of this polymorph in PHs (10–13 mol%) and POs (>10 mol%) is instead explained first by a decreased segmental mobility in the relatively low range of T_cs required for crystallization of these two copolymers. We notice that the only instances of significant γ crystallization at T_cs in the 30–50 °C range involve PE or PB copolymers with high comonomer content for which T_g is relatively low and the availability of crystalline sequences is higher due to the inclusion of the comonomer. A second explanation is morphological. As the co-units are excluded from the crystals, only small crystallites of limited extension in length and width develop at high comonomer contents. Taking the postulate presented by Lotz that branching from the α phase requires a smooth (010) face ≳100 Å [31], as the crystallites become thinner and more segmented with increasing co-unit content of the excluded type, the required surface length to allow epitaxial γ branching no longer can develop.

Degrees of crystallinity were also estimated from the diffractograms of Fig. 6, after subtraction of the amorphous halo. For samples that contained a fraction of crystallites formed during quenching at room temperature, the WAXD crystalline area was corrected by the ratio of the area of the melting peak above T_c over the total melting area (including the quenching peak). These data obtained after isothermal crystallization give a measure of the kinetic effect in building crystallinity, and thus, of the comonomer as a defect in restricting crystalline packing. To minimize overlapping, the data for PE and PB series are given in Fig. 9a and for PH and PO in Fig. 9b for copolymers with >5 mol% comonomer. Despite the participation of the co-unit in the crystals, the decrease in crystallinity for PEs and PBs with increasing T_c and with increasing comonomer indicates that both comonomers are defects that restrict crystallinity. However, at a matched composition the absolute crystallinity value differs greatly between PBs and PEs. All PB copolymers develop between 50 and 45% crystallinity at the fastest crystallizations, while in the same comonomer range the maximum crystallinity developed by PEs decreases from 45% to 15%, pointing out that the increased restrictions to crystallization imposed by the ethylene units follow the general behavior of semicrystalline random copolymers with co-units more discriminated from the crystalline regions. The reason is the kinetic requirements of increasing crystalline sequence length to form a stable crystallite at higher T_cs, or with increasing comonomer, and the depletion in number of these sequences. As the comonomer is

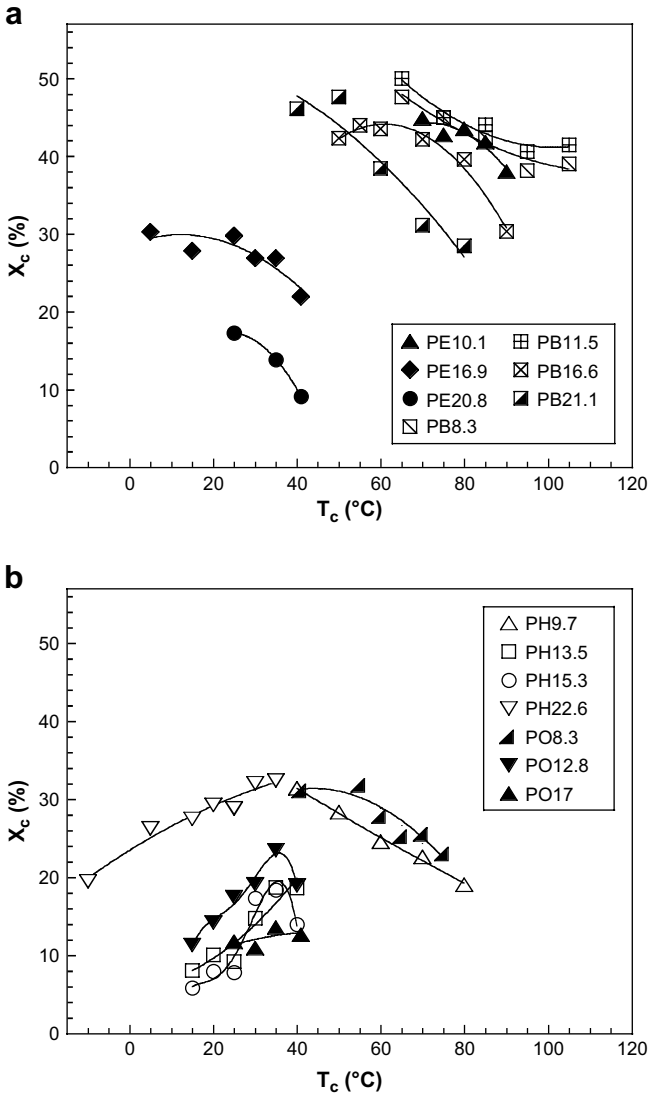

Fig. 9. Percentage crystallinity (X_c) obtained from WAXD of Fig. 7 as a function of crystallization temperature (T_c). (a) Data for PE and PB, (b) data for PH and PO copolymers.

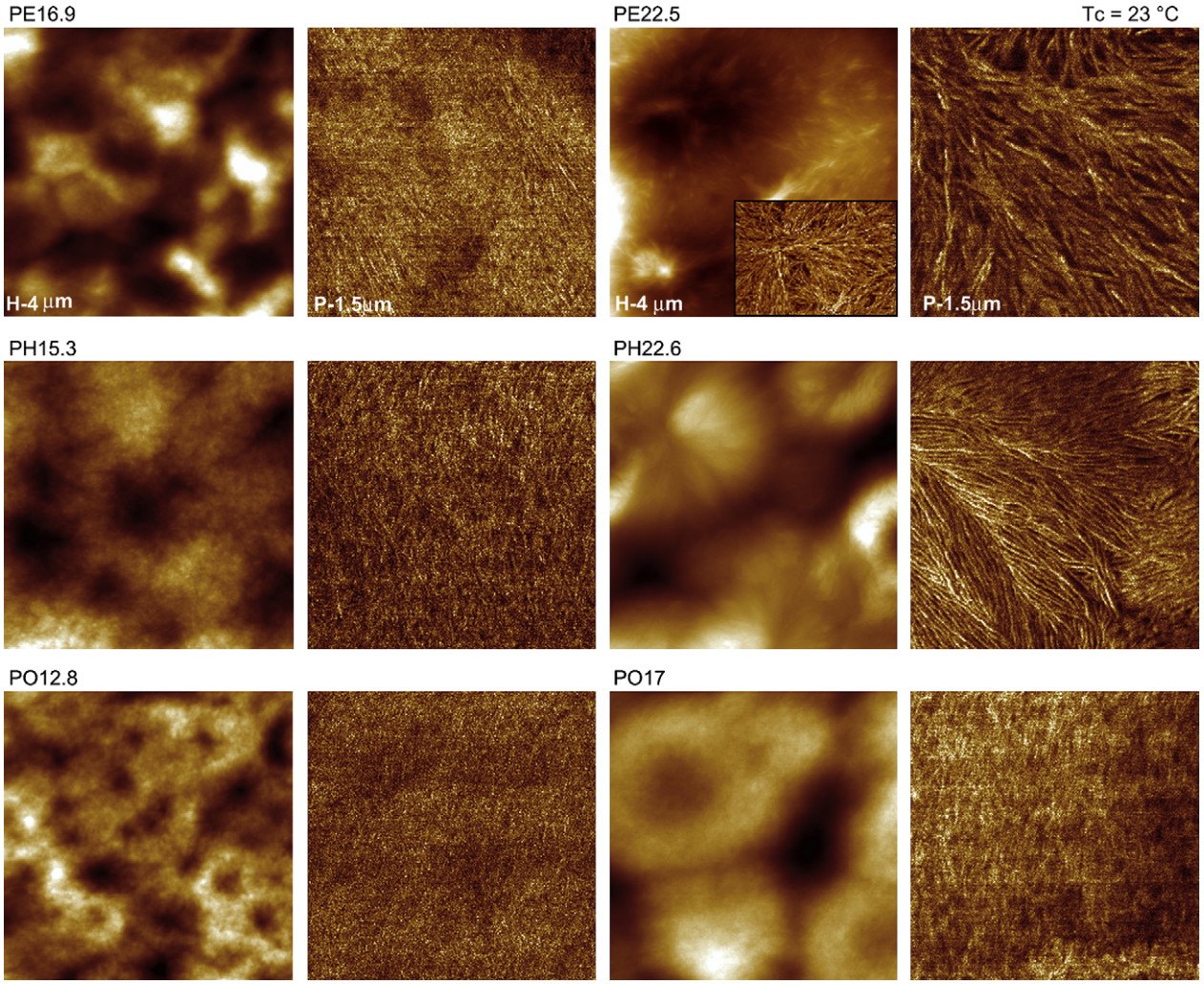

Fig. 10. AFM images of indicated PE, PH and PO copolymers melt crystallized at 23 °C. Topographic and phase images are indicated as H and P respectively, followed by the scan size. The image type and scan size are vertically equivalent. The inset in PE22.5 is the corresponding phase image with a scan size of $3.7 \times 2.6\ \mu m^2$, added to display the axialitic morphology of PE22.5 crystallized at 23 °C.

better incorporated in the crystals, such as for PBs, this number increases, and crystallinity increases correspondingly.

POs and PHs with <10 mol% follow the same decrease of crystallinity with increasing T_c (Fig. 10b). In contrast, the degree of crystallinity for >10 mol% increases with T_c, and appears to level off and further decrease at the highest T_cs, as shown in the diffractograms of PH13.5 and PO12.8 of Fig. 6. We associate this change with the relatively low T_cs needed to observe crystallization in PH and PO copolymers with high co-unit content. Within the sequence limitations in the $T_c > T_{c\ max}$ range, a large fraction of the crystallinity that develops in these copolymers will be favored by the increased segmental transport as T_c increases. Notice that the same trend is found for PH22.6, which develops the trigonal structure in the whole range of T_cs, including crystals formed at $T_c = -10$ °C a temperature only a few degrees above T_g. The crystallinity of PH22.6 increases by two to three folds the value of any PE or PO with >10 mol% comonomer. This is a consequence of the drastic change in crystallization behavior of PH with a large number of 1-hexene co-units participating in the formation of a different, denser phase.

Differences in the crystallization behavior of these iPP copolymers incurred by the role of the comonomer type in packing chain sequences also impact the morphology of the evolving crystallites. The major features are comparatively summarized in the images in Fig. 10 for copolymers with defect compositions between ~13 and ~20 mol%, crystallized at 23 °C. At this T_c, the morphology of any PB copolymer and PEs <15 mol% is featureless due to fast crystallization during cooling prior to reaching T_c, thus not shown. PHs and POs with <15 mol% defects display the same morphology. Even after a relatively slow crystallization, the crystalline morphology of PH15.3 and PO12.8 is composed of multiple thin and short lamellae that aggregate in spherical objects. This morphology parallels the exclusion of the co-units and the restricted number of crystallizable sequences to propagate lamellar crystallites. At 1-hexene >15 mol% the morphology is quite different from the morphology of POs with a comparable comonomer content. The co-crystallization of the comonomer in PE and PH at the ~20 mol% level allows formation of long lamellae of 94 ± 7 Å and 122 ± 9 Å thick respectively, that aggregate into large open spherulites as seen in the images. In contrast, as the 1-octene is not participating in the crystallization, only short and thinner crystallites (~75 Å) can develop in POs at comonomer levels >10 mol%.

4. Conclusions

A comparative analysis of the isothermal crystallization kinetics of four sets of metallocene-made random iPP based copolymers with ethylene, 1-butene, 1-hexene, and 1-octene as co-units

(<21 mol%) has substantiated differences in partitioning of the different comonomer types between the crystalline and non-crystalline regions. Crystallization kinetics coupled with studies of the developing polymorphs, the unit cell expansion, differences in crystalline morphology and melting behavior have also revealed the role of the comonomer type, and content, in developing the copolymer crystalline structure in the nucleation and in the diffusion-controlled regimes.

Fixing comonomer content and T_c, the variation of the rate parallels the partitioning of the co-unit, as a defect, between crystalline and non-crystalline regions. The crystallization of PBs is faster than in matched PEs, and both types present faster rates than those of PH or POs with analogous defect content. In a co-unit range <13 mol% PH and POs have the same crystallization rates, indicative of the same crystallizable sequence length distribution and of the same behavior with respect to the participation of the co-unit in the crystal. Since the 1-octene does not enter the crystal lattice, the 1-hexene units must also be excluded in copolymers with $\lesssim$13 mol% comonomer. This conclusion is supported by solid-state NMR from the absence of residues associated with the branch in the crystalline spectra of PH (<13 mol%) and PO copolymers, by an analogous polymorphic, unit cell expansion, and melting behavior, and by a similar crystalline morphology. Thin crystallites of reduced lateral extension contrast with longer, better-organized lamellae developed by copolymers with co-crystallizable units. The crystallization rates of PHs >15 mol% are significantly higher than for matched POs due to the accommodation in the crystals of a large number of 1-hexene units at this relatively high co-unit level. It is perceived that the crystallization of PH >15 mol% develops by packing comonomer-rich segments, more abundant in the chain at this co-unit level, instead of long isotactic sequences as is the case for PHs and POs with <15 mol%.

In the nucleation-driven crystallization range, or at T_cs $> T_{c\ max}$, the kinetics are governed by undercooling, and thus by the co-crystallizability of the co-unit with the propene unit. Therefore, the values of the rates follow a trend led by the copolymer with the longest crystallizable sequence length, i.e., PB > PE > PH = PO at <13 mol% or PB > PE > PH > PO for >13 mol%. However, the variation of the rates of copolymers with the same molecular weight at $T_c < T_{c\ max}$ is driven by melt segmental dynamics that follow the T_g of each copolymer. The impact of T_g on the crystallization rate is important, especially at the highest co-unit contents. The T_gs of PHs with >15 mol% are >20 °C higher than the T_g values of matched POs, therefore at $T_c < T_{c\ max}$, although the 1-hexene also participates in the crystallites, the PH rates are lower than those of matched POs due to restricted segmental transport.

Lack of development of the γ polymorph in PH and PO copolymers with comonomer contents between 10 and 15 mol% is not due to the inclusion of the comonomer and expansion of the lattice, as previously suggested, but rather due to a decreased segmental mobility and the formation of thin α crystallites too short to enable homo-epitaxial γ branching.

Acknowledgements

Funding of this work by the National Science Foundation, Grant DMR-0503876, is gratefully acknowledged. We acknowledge Drs. S. Kacker and P.S. Ravishankar of the ExxonMobil Co. for synthesis, T_g data and solution NMR characterization of these copolymers and Dr. B. Monrabal of PolyChar for CRYSTAF profiles. The input of one reviewer who pointed out restricted mobility as a possible reason for lack of formation of the γ polymorph in PH and PO copolymers with comonomer contents between 10 and 15 mol% is appreciated. We also acknowledge the technical assistance of Dr. E. Lockner of MARTECH at FSU with X-ray measurements and Y. Chiari and R. Fu (NHMFL) with collection of NMR spectra.

Appendix. Supporting information

The supplementary material associated with this article can be found in the online version at, doi:10.1016/j.polymer.2008.10.032.

References

[1] Pasquini N, editor. Polypropylene handbook. Hanser Gardner; 2005.
[2] Galli P, Vecellio G. Prog Polym Sci 2001;26:1287–336.
[3] Hosier IL, Alamo RG, Esteso P, Isasi JR, Mandelkern L. Macromolecules 2003;36:5623–36.
[4] De Rosa C, Auriemma F, Ruiz de Ballesteros O, Resconi L, Camurati I. Chem Mater 2007;19:5122–30.
[5] Jeon K, Chiari YL, Alamo RG. Macromolecules 2008;41:95–108.
[6] Arnold M, Henschke O, Knorr J. Macromol Chem Phys 1996;197:563–73.
[7] Hosoda S, Hori H, Yada K, Nakahara S, Tsuji M. Polymer 2002;43:7451–60.
[8] De Rosa C, Auriemma F, Ruiz de Ballesteros O, Resconi L, Camurati I. Macromolecules 2007;40:6600–16.
[9] De Rosa C, Auriemma F, Ruiz de Ballesteros O, De Luca D, Resconi L. Macromolecules 2008;41:2172–7.
[10] De Rosa C, Auriemma F, Talarico G, Ruiz de Ballesteros O. Macromolecules 2007;40:8531–2.
[11] Poon B, Rogunova M, Hiltner A, Baer E, Chum SP, Galeski A, et al. Macromolecules 2005;38:1232–43.
[12] Mehta AK, Chen MC, McAlpin JJ. In: Benedikt GM, Goodall BL, editors. Metallocene-catalyzed polymers: materials, properties, processing and market. New York: Plastic Design Library; 1998. p. 261.
[13] Kaminsky W, Külper K, Brintzinger HH, Wild FRWP. Angew Chem Int Ed Engl 1985;24:6.
[14] Alamo RG, Blanco JA, Agarwal P, Randall JC. Macromolecules 2003;36:1559–71.
[15] Brückner S, Meille SV. Nature (London) 1989;340:455–6.
[16] Turner-Jones A, Aizlewwod JM, Beckett DR. Makromol Chem 1964;75:134.
[17] GRAMS. Thermo Fisher Scientific; 2006.
[18] VanderHart DL, Alamo RG, Nyden MR, Kim M-H, Mandelkern L. Macromolecules 2000;33:6078–93.
[19] Alamo RG, VanderHart DL, Nyden MR, Mandelkern L. Macromolecules 2000;33:6094–105.
[20] Nyden MR, Vanderhart DL, Alamo RG. Comput Theor Polym Sci 2001;11:175–89.
[21] De Rosa C, Auriemma F, Corradini P, Tarallo O, Dello Iacono S, Ciaccia E, et al. J Am Chem Soc 2006;128:80–1.
[22] Lotz B, Ruan J, Thierry A, Alfonso GC, Hiltner A, Baer E, et al. Macromolecules 2006;39:5777–81.
[23] Kissin YV, Brandolini AJ. Macromolecules 1991;24:2632–3.
[24] Alamo RG, Kim M-H, Galante MJ, Isasi JR, Mandelkern L. Macromolecules 1999;32:4050–64.
[25] Dlubek G, Bamford D, Rodriguez-Gonzalez A, Bornemann S, Stejny J, Schade B, et al. J Polym Sci Polym Phys Ed 2002;40:434–53.
[26] Alamo RG, Ghosal A, Chatterjee J, Thompson KL. Polymer 2005;46:8774–89.
[27] Chiary YL, Vadlamudi M, Chella R, Jeon K, Alamo RG. Polymer 2007;48:3170–82.
[28] Flory PJ. Trans Faraday Soc 1955;51:848.
[29] Sanchez IC, Eby RK. Macromolecules 1975;8:638–41.
[30] Turnbull D, Fischer JC. J Chem Phys 1949;17:71–3.
[31] Lotz B. J Macromol Sci Part B 2002;41:685–709.